:PAGEversion9R;

K2 Compuscript [compuscript] - fot230 /data/journal/bioc bioc.b bioc2528.k root Thu Feb 11 12:21:17 1999 full terminal narrow nolist laser paper newhyph port cols:1 /data/K2/bin/seta ul:3000 priority:10

ELSEVIER

Biophysical Chemistry 76 (1999) 117–132

Biophysical Chemistry

Gangliosides asymmetrically alter the membrane order in cultured PC-12 cells

B. Ravichandra, Preeti G. Joshi*

Department of Biophysics, National Institute of Mental Health and Neurosciences, Hosur Road, Bangalore 560-029, India

Received 19 August 1998; received in revised form 19 November 1998; accepted 19 November 1998

Abstract

Exogenous gangliosides readily associate with the cell membranes and produce marked effects on cell growth and differentiation. We have studied the effect of bovine brain gangliosides (BBG) on the membrane dynamics of intact cells. The structural and dynamic changes in the cell membrane were monitored by the fluorescence probes DPH, TMA-DPH and laurdan. Incorporation of BBG into the cell membrane decreased the fluorescence intensity, lifetime and the steady state anisotropy of TMA-DPH. Analysis of the time resolved anisotropy decay by wobbling in the cone model revealed that BBG decreased the order parameter, and increased the cone angle without altering the rotational relaxation rate. The fluorescence intensity and lifetime of DPH were unaffected by BBG incorporation, however, a modest increase was observed in the steady state anisotropy. BBG incorporation reduced the total fluorescence intensity of laurdan with pronounced quenching of the 440-nm band. The wavelength sensitivity of generalized polarization of laurdan manifested an ordered liquid crystalline environment of the probe in the cell membrane. BBG incorporation reduced the *GP* values and augmented the liquid crystalline behavior of the cell membrane. BBG incorporation also influenced the permeability of cell membranes to cations. An influx of Na^+ and Ca^{2+} and an efflux of K^+ was observed. The data demonstrate that incorporation of gangliosides into the cell membrane substantially enhances the disorder and hydration of the lipid bilayer region near the exoplasmic surface. The inner core region near the center of the bilayer becomes slightly more ordered and remains highly hydrophobic. Such changes in the structure and dynamics of the membrane could play an important role in modulation of transmembrane signaling events by the gangliosides.

Keywords: Gangliosides; PC-12 cells; Membrane dynamics; TMA-DPH; Laurdan; Fura-2

1. Introduction

Gangliosides are sialic acid-containing glycosphingolipids present in the plasma membrane of mammalian cells and are particularly abundant in neuronal cells. They are asymmetrically located in the outer leaflet of the plasma membrane with hydrophilic oligosaccharide moiety protruding from the extracellular surface and the hydrophobic ceramide portion inserted into the lipid bilayer [1,2]. Gangliosides added exogenously to the culture media are taken up by a variety of

*Corresponding author. Tel.: +91 080 6642121 ext. 271; fax: +91 080 6631830; e-mail: pgjoshi@nimhans.kar.nic.in

0301-4622/99/$ - see front matter
PII: S0301-4622(98)00222-1

cells and associate with their plasma membrane without a change in their chemical nature [3–5]. When inserted into the cell membrane gangliosides produce striking effects on cell growth and differentiation in neuronal cells. They promote neurite outgrowth in primary cultures of neurons and a variety of clonal cell lines including PC-12 cells [6–8]. Gangliosides also facilitate the repair of the nerve cells in various paradigms of nerve damage of traumatic, metabolic, or toxic origin [9,10]. They protect neurons in culture as well as in intact animals against the neurotoxicity elicited by glutamate [11,12]. Monosialo ganglioside GM_1 protects PC-12 cells from apoptotic death due to withdrawal of neurotrophic factors [13]. Recent studies suggest that gangliosides exert the neurotrophic and neuroprotective effects by modulation of some important transmembrane signaling processes. It has been shown that in different cell types gangliosides can alter the activities of protein kinases [13–15], levels of intracellular Ca^{2+} [16–19] and cAMP [20]. Gangliosides have also been shown to induce the breakdown of phosphoinositides in neuro-2a cells [21] and inhibition of nitric oxide synthase in rat brain homogenates [22]. In PC-12 cells, GM_1 together with nerve growth factor recruits a Ca^{2+}-dependent protein kinase [23,24]. Short-term treatment of PC-12 cells with gangliosides has been shown to enhance the depolarization-induced Ca^{2+} influx through dihydropyridine sensitive Ca^{2+} channels and enhance the activity of Ca^{2+}-dependent protein kinase [17].

The activity of many membrane proteins involved in signal transduction, such as receptors and ion channels is regulated by specific lipid–protein interactions and membrane dynamics plays a pivotal role in such lipid–protein interactions [25–27]. The translational, vertical and rotational motion of all membrane proteins as well as the conformation and the corresponding activation of channels and receptors are controlled by membrane dynamics. These lipid–protein interactions are probably responsible for the fine control of signal transduction steps in the cell membrane [24,28–30]. It is evident that exogenously added gangliosides modulate several transmembrane signaling events. To the best of our knowledge the effects of gangliosides on the membrane dynamics of cells has not been studied. Some studies have been performed earlier in model membranes composed of phospholipids and gangliosides and show that gangliosides decrease the membrane fluidity in liposomes [31–33]. In this communication we present the effects of gangliosides on the membrane of intact PC-12 cells. Three different fluorescence probes with their fluorescence moieties localizing in distinct regions of the lipid bilayer were used to monitor the structural and dynamic changes in the plasma membrane. The fluorescence moiety of the hydrophobic molecule 1,6-diphenyl-1,3,5-hexatriene (DPH) localizes near the center of the hydrocarbon core of the membranes. Whereas 1,(4-trimethylammonium),6-diphenyl-1,3,5-hexatriene (TMA-DPH) due to its positive charge anchors to the exoplasmic leaflet with its fluorescent moiety situated in the diacyl chain region of lipids. The lauric acid tail of 6-dodecanoyl-2-dimethylaminonaphthalene (laurdan) anchors into the membrane and the fluorescence moiety naphthalene is located in the interfacial region at the level of phospholipid glycerol backbone. The changes in intracellular ion concentrations were detected by fluorescence probes Fura-2, SBFI, PBFI which preferentially bind Ca^{2+}, Na^{+} and K^{+}, respectively. We report that exogenously added gangliosides produce marked structural and functional changes in the plasma membrane of intact cells. We also found that the ganglioside effects described in model membranes are not absolutely extendible to the cells maintained under the physiological conditions.

2. Materials and methods

Purified bovine brain ganglioside mixture (BBG) was obtained from Sigma Chemical Co. St. Louis, MO. (USA). Fluorescent probes DPH, TMA-DPH, laurdan, Fura-2 acetoxymethyl ester (Fura-2/AM), sodium binding benzofuran isophthalate acetoxymethyl ester (SBFI/AM) and potassium binding benzofuran isophthalate acetoxymethyl ester (PBFI/AM) were purchased from Molecular Probes Inc. Eugene, OR (USA). RPMI 1640 medium was purchased from Hi Media, Bombay (India) and fetal calf serum from

Biological Industries (Israel). Horse serum was prepared in our laboratory.

2.1. Cell culture

PC-12 cells were obtained from National Center for Cell Sciences Pune, India. Cells were grown in plastic culture flasks (Corning) containing RPMI 1640 medium supplemented with 2 g/l sodium bicarbonate, 5% fetal calf serum, 10% horse serum, 50 000 units/l benzyl penicillin and 3500 units/l streptomycin. Cells were incubated at 37°C in an atmosphere of 5% CO_2 and 95% air. The medium was changed once at 72 h and the experiments were performed at 120 h.

2.2. Labeling of cells with fluorescence probes

The fluorophores were loaded into the cell in suspension. Cells were released from the culture flasks by gentle pipetting, washed with PBS containing 5 mM glucose and were maintained in the same buffer during the following steps. DPH and TMA-DPH were loaded into the cells according to the procedures described by Shinitzky et al. [34] and Petty et al. [35], respectively with some modifications. Briefly, labeling solutions of DPH and TMA-DPH were prepared by slowly adding specific volumes of their stock solutions in dimethyl formamide to a known volume of vigorously stirred PBS containing 5 mM glucose. A known volume of this solution was added to an equal volume of cell suspension containing 2×10^6 cells/ml. In the case of TMA-DPH the cell suspension was gently shaken for 2 min. Then the cells were washed two times to remove the extracellular probe and resuspended in the buffer. For DPH labeling cells were incubated in the labeling buffer for 30 min in the shaker water bath at 30°C, then washed and resuspended in the buffer.

Laurdan was labeled into the cells as described by Parassasi et al. [36]. Cells were suspended in the labeling buffer consisting of 1 μM laurdan, 5 mM glucose and PBS. The cell suspension was incubated for 30 min in the shaker water bath at 30°C, then washed and resuspended in the buffer.

Fura-2, SBFI and PBFI were loaded into the cells in suspension. Cells at a density of 2×10^6 cells/ml were incubated with the acetoxymethyl esters of respective dyes in buffer containing 130 mM NaCl, 5 mM KCl, 1 mM $MgCl_2$, 1 mM $CaCl_2$, 5 mM glucose and 20 mM Tris (pH 7.4). The concentration of Fura-2/AM, SBFI/AM and PBFI/AM in the incubation buffer was 2, 10 and 8 μM, respectively and the dye was mixed thoroughly with pluronic (0.08%) before addition to the buffer. Cells were incubated at 37°C for 30 min with Fura-2/AM and 90 min with SBFI/AM or PBFI/AM in the shaker water bath. Cells were then washed and resuspended in the same buffer.

2.3. Treatment of cells with BBG

BBG is a mixture of gangliosides extracted from bovine brain. Typically the mixture contains monosialoganglioside GM_1, disialogangliosides GD_{1a} and GD_{1b} and trisialoganglioside GT_{1b}. A stock solution of BBG was prepared in an ethanol-water (1:1) mixture. Aliquots of this stock solution were added to the fluorophore labeled cells to give the desired concentrations of BBG in the medium. Cells were incubated with BBG for 15 min at room temperature prior to the fluorescence measurements.

2.4. Cell viability

Effect of fluorescence probes and BBG on the viability of cells was assessed by the trypan blue exclusion method. DPH, TMA-DPH and laurdan did not affect the viability of cells within the experimental time. Similarly BBG addition also did not affect the cell viability.

2.5. Fluorescence microscopy

The labeled cells were examined in a Leica DMRB fluorescence microscope equipped with a CCD camera. Video signals were recorded and stored in the computer using Q-Win 500 + image analysis software. Photographs were taken from the monitor screen with a Nikon 35 mm camera. A 50 W mercury lamp was used to illuminate the samples. The excitation filter was 360 nm and the emission barrier filter was 420 nm.

2.6. Steady state fluorescence measurements

The fluorescence spectra and steady state anisotropy were measured with SLM 8000C spectroflurometer. The bandwidth of excitation and emission monochromators was 2 nm while recording the fluorescence spectra. For the measurements of anisotropy Glan Thompson calcite prism polarizers were placed in the excitation and emission paths and the emitted light was selected by a cut off filter. Samples were excited with vertically polarized light and vertically (I_{vv}) and horizontally (I_{vh}) polarized fluorescence intensities were measured simultaneously using the T-geometry optical path. The anisotropy was calculated using the relationship:

$$r = (I_{vv} - GI_{vh})/(I_{vv} + 2GI_{vh}) \quad (1)$$

Where G is the correction factor given by $G = I_{hv}/I_{hh}$. G was determined by measuring the fluorescence intensities I_{hv} and I_{hh} using the horizontally polarized exciting light.

All the fluorescence measurements were performed in cell suspensions at a density of 1×10^6 cells/ml. The optical density of labeled cell suspensions was < 0.15 at the respective excitation wavelengths used for fluorescence measurements, thus the inner filter effects are expected to be negligible. The fluorescence spectra depicted here are corrected for the autofluorescence and light scattered by cells. Autofluorescence from unlabelled cells at the same density was subtracted from the fluorescence spectrum of labeled cells. In the case of BBG treated samples, an appropriate blank control was also treated with BBG and the signal due to autofluorescence and scattered light was subtracted from the sample fluorescence. Anisotropy values were calculated after subtracting the appropriate blanks. All the experiments were performed at room temperature.

Since the stock solution of BBG was prepared in an ethanol–water mixture, control experiments were performed to examine the effect of ethanol on the fluorescence parameters of the labeled cells. Equivalent aliquots of ethanol–water did not elicit any change in the fluorescence intensity or the anisotropy of DPH and TMA-DPH labeled cells. Similarly no change was seen in the laurdan fluorescence.

2.7. Time resolved fluorescence measurements

The decay of fluorescence intensity and anisotropy was measured by single photon counting method using the Edinburgh CD 900 spectrofluorometer as described earlier [37]. The light source was a N_2 discharge lamp operated at a pressure of 1 bar. The bandwidth for excitation and emission monochromators was 4 nm. For each sample decay curve data were acquired to give a peak count of 5000 and a corresponding lamp profile was collected using a scattering solution. To measure the decay of fluorescence anisotropy Glan Thompson calcite prism polarizers were placed in the excitation and emission monochromators. Samples were excited with vertically polarized light. Decay of vertically $I(t)_{vv}$ and horizontally $I(t)_{vh}$ polarized fluorescence intensities were measured by toggling the emission polarizer between vertical and horizontal positions and simultaneously acquiring the data in two memory segments of a multichannel analyzer (MCA). The simultaneous toggling of emission polarizer and switching to the corresponding MCA memory segments was automatically controlled with a dwelling time of 60 s. The decay of anisotropy was generated using Eq. (1).

2.8. Analysis of fluorescence intensity and anisotropy decay

The fluorescence intensity decay is represented by a sum of multi-exponentials, such as

$$I(t) = I_0 \sum e^{-t/\tau i} \quad (2)$$

which was analyzed by non-linear least square deconvolution procedure [38]. The best fit was judged by χ^2 and residuals. The fractional intensity (f_i) of each component is given by

$$f_i = \alpha_i \tau_i / \sum_i \alpha_i \tau_i \quad (3)$$

where α is the pre-exponential factor and τ is the decay time.

The decay of fluorescence anisotropy was analyzed according to the wobbling in cone model [39,40]. The fluorophore in the membrane is considered to be in a hindered environment and its orientational motion is described by the wobbling confined within a cone around the normal of the membrane. The decay of the fluorescence anisotropy of the fluorophore in the hindered environment is represented by

$$r(t) = (r_0 - r_\infty)e^{-t/\phi} + r_\infty \quad (4)$$

where r_0 is the anisotropy at $t = 0$, r_∞ is the limiting anisotropy and ϕ is the rotational relaxation time for the wobbling diffusion within the cone. The relationship between the cone angle and the limiting anisotropy is given by:

$$r_\infty/r_0 = 1/4[\cos\theta_c(1 + \cos\theta_c)]^2 \quad (5)$$

The limiting anisotropy is related to the membrane order parameter (S) by equation

$$r_\infty/r_0 = S^2 \quad (6)$$

2.9. Generalized polarization measurements

The fluorescence spectra of laurdan display characteristic features related to the phase state and dynamics of its environment. Based on these properties the generalized polarization of laurdan is given by [44,45]

$$GP = (I_B - I_R)/(I_B + I_R) \quad (7)$$

where I_B and I_R are the fluorescence intensities at the blue and red edges of the spectrum, respectively. Fluorescence intensities at 440 and 490 nm were used to calculate GP_{ex} whereas GP_{em} was calculated using the excitation wavelengths of 350 and 390 nm.

2.10. Measurement of intracellular ion concentration

The intracellular concentration of Na^+, K^+ and Ca^{2+} was measured using their respective fluorescent indicators namely SBFI, PBFI and Fura-2. Cells were loaded with respective dyes as described above. Intracellular ion concentrations were determined by a ratiometric method as described earlier [41]. The fluorescence intensity ratios were calibrated by measuring the fluorescence in permeabilized cells at saturating or minimal concentrations of respective ions. Permeabilization was achieved by digitonin, gramicidin or valinomycin in case of Ca^{2+}, Na^+ and K^+ ions, respectively.

3. Results

3.1. Labeling and localization of TMA-DPH, DPH and laurdan in cells

In preliminary experiments performed to optimize the labeling of fluorescence probes in PC-12 cells the fluorescence intensity was measured as a function of labeling time and probe concentration (data not shown). In case of TMA-DPH maximum intensity was obtained within 2 min, whereas, the fluorescence intensity of DPH and laurdan constantly increased with time plateauing at approximately 30 min. An increase in the probe concentration was accompanied by proportional increase in the fluorescence intensity of labeled cells up to 2 μM of TMA-DPH and DPH followed by a decrease in intensity at higher probe concentrations. This diminution of intensity is attributed to self quenching due to aggregation of probe molecules in cells. The quenching was observed above 1 μM in laurdan labeled cells. Thus in following experiments cells were labeled by incubation with 2 μM of TMA-DPH for 2 min, 2 μM of DPH for 30 min and 1 μM of laurdan for 30 min.

The cellular localization of the fluorescence probes was characterized by fluorescence microscopy. The fluorescence photomicrographs of the labeled cells are depicted in Fig. 1. As already reported by other authors [42,43], high quality photomicrographs could not be obtained due to the rapid photobleaching of TMA-DPH and DPH. However, the demarcation of fluorescence was convincingly clear when directly observed with the microscope. Panel (a) shows the photomicrograph of PC-12 cells immediately after labeling

with DPH. The fluorescence intensity was essentially associated with the plasma membrane with slightly diffused boundaries. It was noted that no fluorescence was exhibited from the intracellular region indicating that intracellular membranes were not labeled, but the fluorescence profile of cells changed with time. Up to 20 min the fluorescence was clearly seen on the periphery of cells whereas after 30 min the fluorescence was localized mainly in the intracellular region (panel b) indicating the migration of DPH from the plasma membrane to the intracellular membranes. Therefore all the experiments with DPH labeled cells were performed within 15 min after labeling. As shown in panel (c) the fluorescence intensity of TMA-DPH was associated with well defined periphery of cells and remained at the same location even after 1 h (panel d). These results provide evidence that TMA-DPH intercalates only in the plasma membrane of PC-12 cells and does not get internalized within the experimental time. The fluorescence photomicrographs of laurdan labeled cells could not be obtained due to the low intensity and rapid photobleaching of the probe. Under direct observation the fluorescence was seen distinctly on the plasma membrane without labeling of intracellular compartments.

3.2. Fluorescence spectra and decay times of TMA-DPH

The fluorescence spectra of TMA-DPH in PC-12 cells before and after BBG addition are depicted in Fig. 2. Gangliosides diminished the fluorescence intensity in a concentration-dependent manner. Exogenously added gangliosides are known to incorporate into the plasma membrane of a variety of cell types, however, a significant fraction will be present as micellar structures in the extracellular medium. Any residual fluorescent probe in the extracellular medium can bind

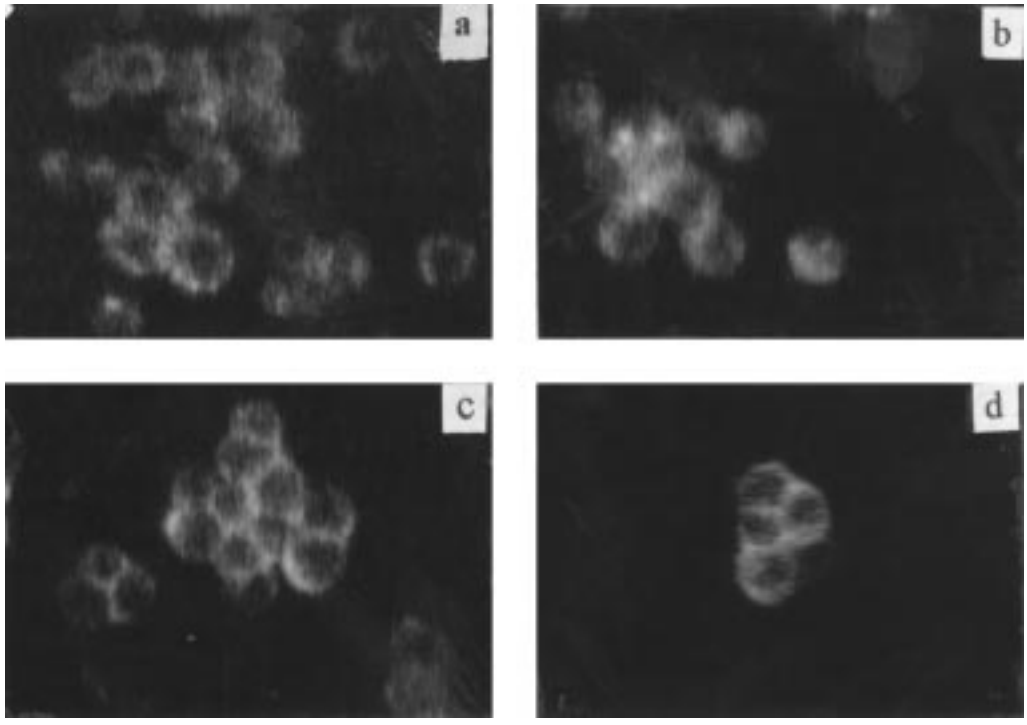

Fig. 1. Fluorescence photomicrographs of DPH and TMA-DPH labeled PC-12 cells. Cells were loaded in suspension with 2 μM of DPH or TMA-DPH. Upper panels show DPH labeled cells (a) 1 min and (b) 30 min after labeling. Lower panel shows TMA-DPH labeled cells (c) 1 min and (d) 60 min after labeling. All photomicrographs were taken at a magnification of 600 $\times$.

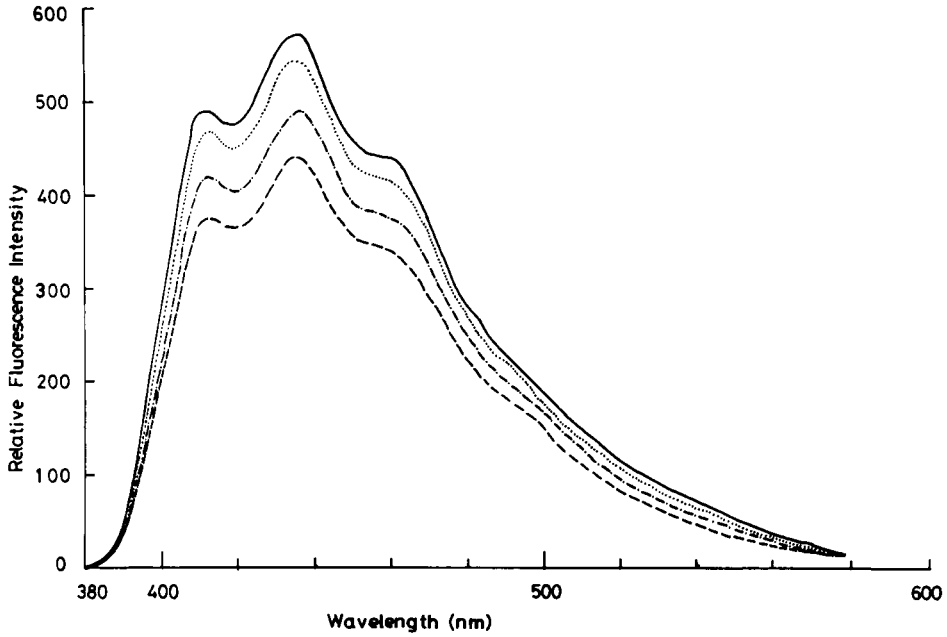

Fig. 2. Emission spectra of TMA-DPH in PC-12 cells before and after BBG treatment. Cell suspension at a density of 1×10^6 cells/ml was excited with 337 nm. The fluorescence intensity in cells treated with 50 (· · ·), 100 (– · –) and 200 (– – –) μg/ml of BBG is shown relative to the intensity in (———) untreated cells.

to the micelles and can influence the fluorescence measurements on the membrane bound probes. Therefore extreme care was taken to remove the extracellular probe before the addition of gangliosides. The decrease in the fluorescence intensity of TMA-DPH in cells is due to the partitioning of BBG into the plasma membrane of cells as incorporation of TMA-DPH into the micelles markedly increased the fluorescence intensity (data not shown).

The fluorescence decay curves of TMA-DPH in PC-12 cells before and after the addition of BBG are depicted in Fig. 3. In both the cases a best fit was obtained for a double exponential decay. The lifetime values, their fractional contributions and the average lifetimes are given in Table 1. BBG addition caused a decrease in both the lifetime components. The fractional contributions were not affected up to the BBG concentrations of 100 μg/ml whereas at 200 μg/ml, the contribution

Table 1
Fluorescence lifetime of TMA-DPH in PC-12 cells treated with BBG

BBG Conc. (μg/ml)	Lifetime		Fractional intensity		τ_{av} ns
	τ_1	τ_2	f_1	f_2	
0	7.14 ± 0.36	2.77 ± 0.29	0.77 ± 0.05	0.23 ± 0.05	6.22 ± 0.29
50	6.67 ± 0.22	2.29 ± 0.09	0.75 ± 0.03	0.25 ± 0.03	5.65 ± 0.15[a]
100	6.32 ± 0.23[a]	1.93 ± 0.42	0.74 ± 0.05	0.26 ± 0.05	5.22 ± 0.09[a]
200	6.14 ± 0.09[a]	1.90 ± 0.03	0.66 ± 0.03	0.34 ± 0.03	4.71 ± 0.11[a]

Each data point is the mean ± S.D. from four experiments.
[a] Significantly different than control (0 BBG conc.) at $P < 0.005$.

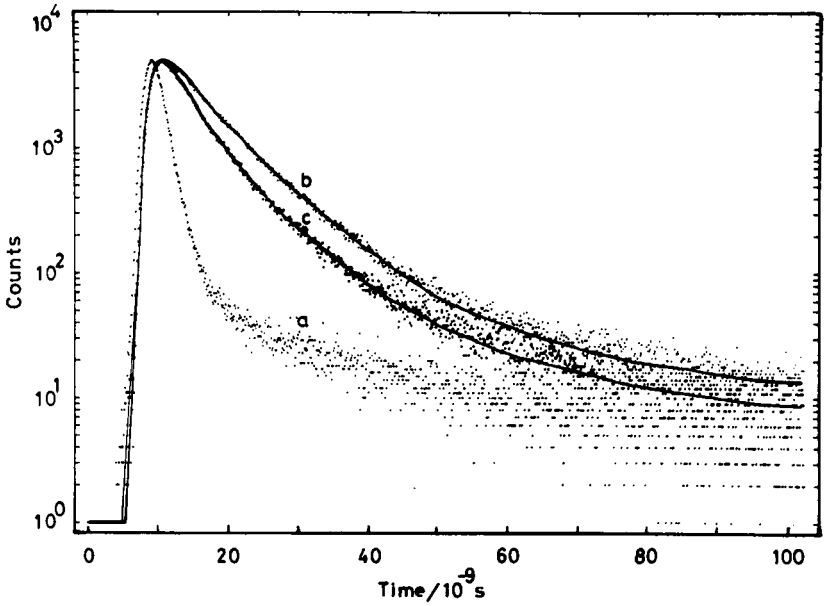

Fig. 3. Fluorescence decay of TMA-DPH in cells. The excitation and emission wavelengths were 337 and 415 nm respectively; (a) lamp profile, (b) untreated cells and (c) cells treated with 200 μg/ml of BBG. Dots represent the experimental data and solid line is the fitted curve.

of the shorter component increased slightly. A significant decrease was observed in the average lifetime of TMA-DPH at BBG concentrations of 100 μg/ml or higher. The decrease in the fluorescence intensity and the lifetime indicate that the microenvironment of TMA-DPH becomes more hydrophillic after the incorporation of BBG into the cell membrane as the fluorescence intensity and lifetime of TMA-DPH are known to decrease in the polar solvents.

3.3. Steady state and time resolved anisotropy of TMA-DPH

Steady state and time resolved fluorescence anisotropy of TMA-DPH was measured to assess the effect of BBG on the mobility of the membrane lipids. The steady state anisotropy of TMA-DPH in PC-12 cells was found to be 0.279 ± 0.001 and addition of BBG reduced the anisotropy value in a concentration-dependent manner. The change in the steady state anisotropy as a function of BBG concentration is shown in Fig. 4. Addition of 50 μg/ml BBG significantly reduced the fluorescence anisotropy value. Increasing the BBG concentration to 100 and 200 μg/ml caused a further decrease though smaller in magnitude. The non-linearity of anisotropy change with BBG concentration could be due to the limited capacity of gangliosides to partition in to the cell membrane. The anisotropy of TMA-DPH in BBG micelles was found to be 0.294 ± 0.002 $(n = 4)$ which is significantly higher than that in the cell membrane. Thus the observed decrease in the anisotropy after the addition of BBG is due to the incorporation of gangliosides into the cell membrane.

Time-dependent fluorescence anisotropy of TMA-DPH was measured to further investigate the effect of BBG on the dynamics of the lipid bilayer. The decay of fluorescence anisotropy was analyzed by the wobbling in cone model as described above and the best fit was found with a single correlation time. The data are shown in Table 2. Addition of BBG reduced the limiting anisotropy (r_∞) in a concentration-dependent manner. This was reflected as a decrease in the order parameter (S) and an increase in the cone

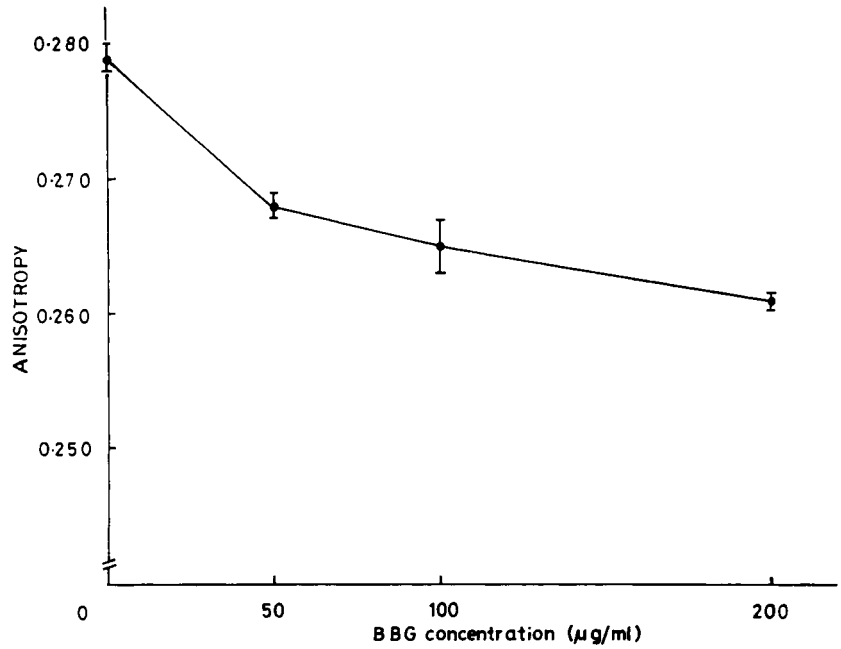

Fig. 4. Steady state anisotropy of TMA-DPH in cells as a function of BBG concentration. Each data point is the mean ± S.D. from five experiments.

angle (θ_c). No significant change was observed in the rotational correlation time (ϕ). The limiting anisotropy (r_∞) and cone angle (θ_c) determine the range and the rotational correlation time (ϕ) determines the rate of the wobbling motion of the probe in the lipid bilayer. Our data show that in BBG treated membranes the range of the wobbling motion of TMA-DPH increases without changing its rotational rate. This indicates a less hindered motion of TMA-DPH in BBG treated membranes.

3.4. Fluorescence lifetime and anisotropy of DPH

The fluorescence properties of DPH are similar to TMA-DPH, however, it localizes in the central hydrophobic region of the lipid bilayer and spans both the leaflets. Interestingly the effects of BBG

Table 2
Limiting anisotropy (r_∞), rotational relaxation time (ϕ), order parameter (S) and cone angle (θ_c) of TMA-DPH in PC-12 cells before and after the addition of BBG

BBG Conc. (μg/ml)	r_∞	ϕ ns	S	θ_c
0	0.260 ± 0.013	3.399 ± 1.225	0.813 ± 0.021	29.46 ± 1.87
50	0.242 ± 0.008[a]	5.222 ± 1.938	0.785 ± 0.014	31.82 ± 1.12
100	0.233 ± 0.015[a]	5.543 ± 1.670	0.769 ± 0.024	33.07 ± 1.96
200	0.207 ± 0.009[a]	4.382 ± 2.382	0.727 ± 0.016[a]	36.36 ± 1.20[a]

Each data point is Mean ± S.D. from five experiments.
[a] Significantly different than control (0 BBG conc.) at $P < 0.005$.

on the fluorescence characteristics of DPH were different than those observed in the case of TMA-DPH. BBG addition did not alter the fluorescence intensity of DPH in the cell membranes. The fluorescence lifetimes of DPH in PC-12 cells were 4.24 ± 2.2 and 9.87 ± 1.03 ns with fractional contributions of 0.21 ± 0.022 and 0.78 ± 0.022, respectively and the average lifetime was 8.83 ± 0.22 ns. BBG addition did not cause any appreciable change in the fluorescence lifetimes. These results suggest that BBG incorporation does not affect the hydration in the inner core region of the membrane. The effect of BBG on the fluorescence anisotropy of DPH was opposite to that observed in TMA-DPH. As depicted in Fig. 5 BBG caused a small increase in the steady state anisotropy of DPH. The change in anisotropy was significant only at BBG concentrations of 100 μg/ml or higher. Time resolved anisotropy experiments could not be performed with DPH due to the technical limitations. Since the fluorescence intensity in DPH labeled cells was low, considerably long data acquisition time was required to generate the anisotropy decay curve and during this time DPH migrates from the plasma membrane as described above. The increase in the steady state anisotropy of DPH implies a more rigid environment of DPH in BBG treated membranes.

3.5. Fluorescence spectra of laurdan

The amphiphilic fluorescent probe laurdan localizes in the interfacial region of the lipid bilayer membranes and its fluorescence intensity is sensitive to the polarity of its environment and the phase of the lipid bilayer [44,45]. Laurdan shows characteristic emission peaks at 440 and 490 nm in the gel and liquid crystalline phases of the phospholipids irrespective of their acyl chain composition and head groups. The emission maxima at 440 nm and 490 nm have been attributed to two different fluorescent species corresponding to non-relaxed and relaxed states of the molecule. Both of these species elicit the excitation peaks at 350 and 380 nm with variation in their relative intensities. The relative population of the non-relaxed and relaxed states depend on the solvation

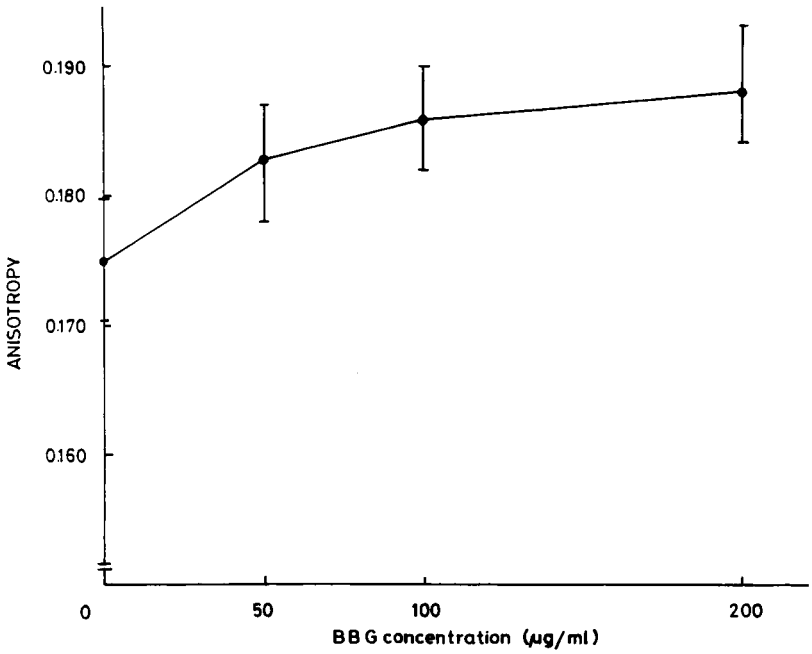

Fig. 5. Steady state anisotropy of DPH in cells as a function of BBG concentration. Each data point is the mean $\pm$ S.D. from five experiments.

of laurdan and the dipolar relaxation of the molecules surrounding the laurdan molecule which in turn depend on the polarity and the phase of the lipid bilayer. Fig. 6 shows the fluorescence excitation and emission spectra of laurdan in PC-12 cells. The fluorescence spectrum exhibited a maximum at 435 nm with a hump at 490 nm and the excitation spectrum elicited the maxima at 350 nm and 380 nm. The emission spectrum of laurdan in PC-12 cells resembles the spectrum reported in K562 cells [36] and in leukocytes [46]. The excitation spectrum shows higher intensity of the 380 nm band as compared to that observed in the liquid crystalline phase of phospholipids. The relative enhancement of the 380 nm band is probably due to the more polar environment of laurdan in PC-12 cells as compared to phospholipids. This conjecture is supported by the fact that when the samples were excited at 390 nm the emission was red, shifted by approximately 3 nm due to the solvent relaxation (data not shown). Enhancement of the red excitation band and red shift in the emission maximum of laurdan in polar solvents has been reported earlier [45].

Addition of BBG caused a decrease in the fluorescence intensity of laurdan without any appreciable shift in the excitation or emission peak positions. In the emission spectrum the diminution of intensity was more pronounced at 440 nm as compared to 490 nm and the half bandwidth of the spectrum increased to 92 nm from 84 nm. Similarly in the excitation spectrum a greater reduction was observed at 380 nm as compared to 350 nm. These results indicate a shift in the population of the two states, i.e. the population of non-relaxed state decreases and the relaxed state increases after the addition of BBG. In earlier studies on phospholipid vesicles it has been shown that similar changes occur in the relative intensities of 390 nm excitation and 440 nm emission bands during the transition from gel phase to liquid crystalline phase [44]. The reduction in the total fluorescence intensity of laurdan after BBG addition can be attributed to increased hydration of the lipid bilayer in the outer leaflet region.

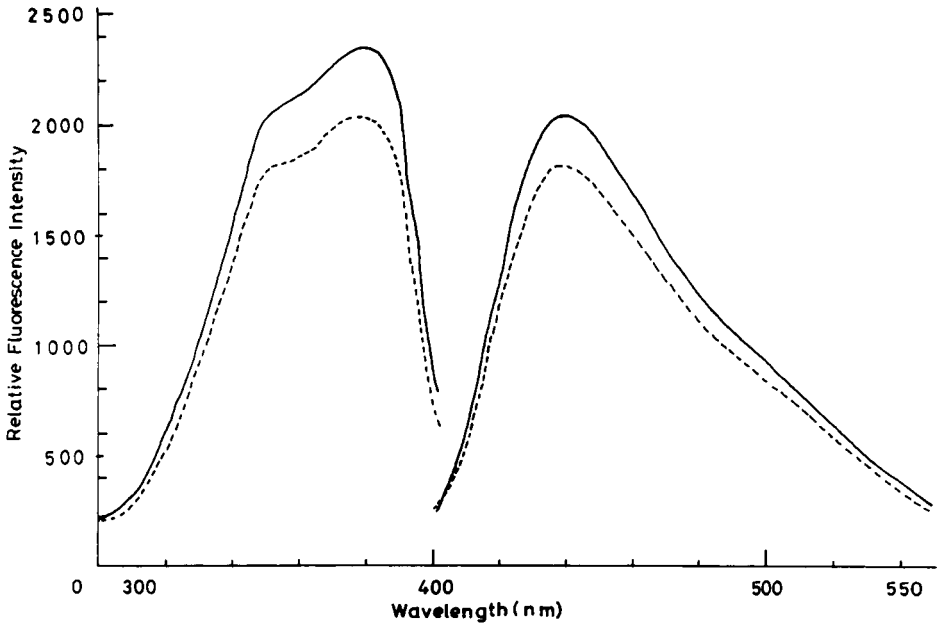

Fig. 6. Excitation and emission spectra of laurdan in PC-12 cells. Samples were excited at 390 nm for recording the emission spectra and emission was monitored at 440 nm for recording the excitation spectra. (——) untreated cells and (· · ·) after treatment with 200 μg/ml of BBG.

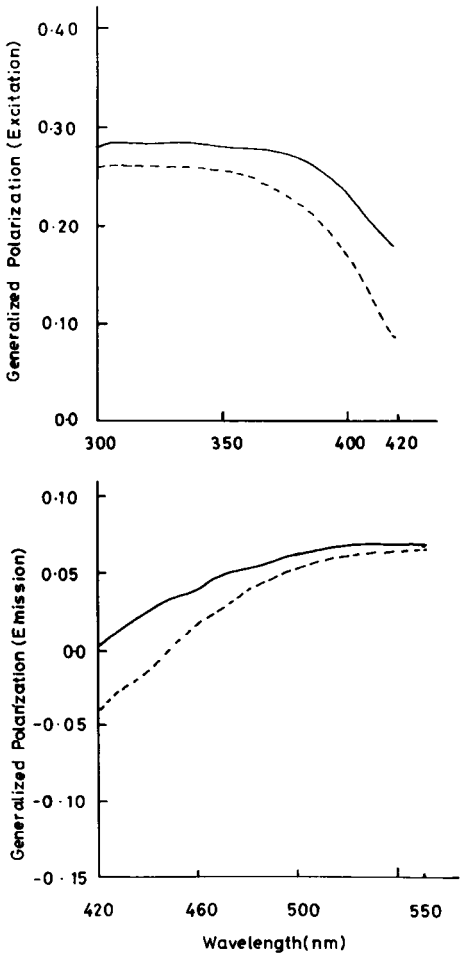

Fig. 7. Generalized polarization spectra of laurdan in untreated cells (———) and cells treated with 200 μg/ml of BBG (· · ·).

This is in agreement with the results obtained with TMA-DPH.

3.6. Generalized polarization of laurdan

Generalized polarization (*GP*) of laurdan in phospholipid vesicles has been shown to explicate their phase behavior. Parassassi et al. [47] have shown that laurdan *GP* in phospholipids exhibit characteristic wavelength dependence in gel, liquid crystalline and mixed phase lipid domains and the *GP* values can be used to quantitate the phase fluctuations in phospholipid bilayers. The excitation and emission *GP* spectra of laurdan in PC-12 cells were constructed and are shown in Fig. 7. The excitation *GP* value was constant up to 370 nm and decreased at longer wavelengths. Similarly emission *GP* values increased up to 475 nm and remained constant at longer wavelengths. This wavelength dependence of excitation and emission *GP* is characteristic of liquid crystalline phase. An opposite behavior is seen in coexisting mixed phase domains and in gel phase *GP* does not show a wavelength dependence [47]. Thus the fluorescence spectra and the *GP* of laurdan show that the PC-12 cell membranes mimic the liquid crystalline phase of phospholipids. This is in conformity with the fluid nature of the cell membranes.

The effect of BBG was well reflected in the excitation and emission generalized polarization of laurdan. Table 3 shows the excitation and emission *GP* values before and after the addition of different concentrations of BBG. Both the excitation and emission *GP* values were reduced by addition of BBG in a concentration-dependent manner. As shown in Fig. 6 BBG addition reduced the *GP* values at all wavelengths and enhanced the wavelength sensitivity of *GP*. In the red and blue edges of excitation and emission spectra, respectively the *GP* changes were more pronounced. These results imply that BBG incorporation augments the liquid crystalline behavior of the cell membrane.

3.7. Permeability of plasma membrane

The structural and dynamic changes in the lipid bilayer may control the permeability of cell mem-

Table 3
Excitation and emission generalized polarization of laurdan in PC-12 cells before and after BBG addition

BBG Conc. (μg/ml)	*GP* Excitation at 390 nm	*GP* Emission at 440 nm
0	0.274 ± 0.011	0.046 ± 0.006
50	0.258 ± 0.008	0.024 ± 0.003
100	0.226 ± 0.019	0.022 ± 0.002
200	0.181 ± 0.043	0.017 ± 0.001

Each data point is Mean ± S.D. from three experiments.

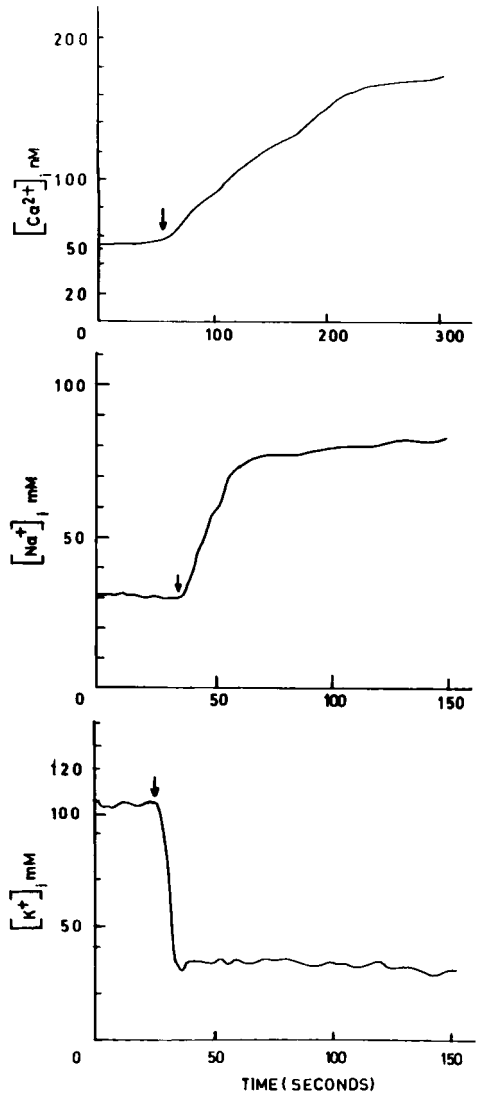

Fig. 8. Effect of BBG on the intracellular concentrations of Ca^{2+}, Na^+ and K^+. Fluorescence intensity of dye loaded cells was monitored at 505 nm by alternately exciting at 340 and 380 nm. BBG (100 μg/ml final concentration) was added at the time indicated by an arrow. Intensity ratio was calculated after subtracting the autofluorescence from cells not loaded with the dye. The data shown here are from a typical experiment repeated five times.

branes. We studied the effect of BBG on cation permeability of the plasma membrane. The intracellular concentrations of Na^+, K^+, and Ca^{2+} in PC-12 cells were 24.66 ± 1.52 mM ($n = 3$), 106 ± 9.60 mM ($n = 3$) and 61.44 ± 9.68 mM ($n = 5$), respectively. As shown in Fig. 8 BBG caused an influx of Na^+ and Ca^{2+} ions and an efflux of K^+ ions bringing their intracellular concentrations to 101.66 ± 8.96 mM, 27.0 ± 5.29 mM and 161.13 ± 14.71 nM, respectively. Interestingly the flux rate was markedly different for the three ions in the order $Na^+ > K^+ > Ca^{2+}$.

4. Discussion

We have studied the structural and functional changes brought about by gangliosides in the plasma membrane of intact PC-12 cells. Our results demonstrate that exogenously added gangliosides significantly modify the ion permeability, polarity, dynamics and phase behavior of the plasma membrane lipid bilayer. The changes in the fluorescence characteristics of three different probes with their fluorescence moieties localized in distinct regions of the lipid bilayer reveal that the structural changes caused by gangliosides are more pronounced near the exoplasmic surface of the bilayer. The opposite effects of BBG on the fluorescence anisotropy of TMA-DPH and DPH reveal that ganglioside incorporation into the membrane results in disorder of the lipid bilayer near the exoplasmic surface but the inner core region becomes more ordered. Time resolved anisotropy provides further information about the rate and the range of the motion of the probe in the bilayer. The decrease in the order parameter and a larger cone angle indicate a less restricted orientational motion of TMA-DPH in the lipid bilayer after BBG incorporation and confirms the disordering effect of gangliosides on the lipid bilayer region near the exoplasmic surface.

Laurdan exhibits characteristic fluorescence spectra and well defined *GP* values in the gel and liquid crystalline phases of a variety of phospholipid vesicles [44,45,47]. The *GP* value does not depend on the type of the polar head groups and the pH between 4 and 10, nevertheless it is sensitive to the packing of the acyl chains in the lipid bilayer and displays a characteristic wavelength dependence in different lipid phases. The fluorescence spectra and *GP* values of laurdan in PC-12 cells suggest an ordered liquid crystalline matrix for the laurdan molecule, which is consis-

tent with the fluid nature of the cell membranes. The wavelength dependence of *GP* was also similar to that reported for homogeneous liquid crystalline phase [47]. The reduction in the *GP* value and the enhancement of its wavelength sensitivity after BBG addition corroborate our inference that gangliosides enhance the orientational mobility of lipids near the exoplasmic surface.

Gangliosides have been shown to decrease the membrane fluidity in phospholipid bilayers [31–33]. Ganglioside GM_1 increased the order parameter of EPR probes 5- and 16-nitroxystearic acid in phospholipid vesicles suggesting decreased mobility of lipid acyl chains in the inner core and near the interfacial region of the bilayer [31]. The dissimilarity of results in phospholipid vesicles and PC-12 cells is possibly due to the difference in the distribution of gangliosides in their lipid bilayers. In phospholipid vesicles gangliosides are added during the vesicle preparation and are expected to be present in both halves of the bilayer whereas in cells they are localized in the exoplasmic leaflet. Secondly the concentration of gangliosides in cell membranes could be much lower than that used in phospholipid vesicles. Thus our data show that the influence of gangliosides described in phospholipid vesicles can not be extrapolated to intact cell membranes.

Our study also revealed that the gangliosides increase the hydration of the lipid bilayer region probed by TMA-DPH and laurdan. The decrease in the fluorescence intensity and lifetime of TMA-DPH indicate a more polar environment for the probe after BBG incorporation. Similarly a decrease in the fluorescence intensity of laurdan was observed although the fluorescence lifetimes did not change (TMA-DPH and laurdan are non-fluorescent in the aqueous medium). No change was observed in the intensity or the lifetime of DPH suggesting that the hydration of lipids was restricted to the bilayer region close to the cell surface.

The above described effects of BBG on the cell membrane can be ascribed to the properties of gangliosides which possess long fatty acid chains and large headgroups. Insertion of the long fatty acyl chains into the membrane is expected to increase the average order in the lipid bilayer, however, our data show paradoxical effects in two different regions of the bilayer. Due to the negative charge and high polarity of headgroups exogenously added gangliosides incorporate only into the outer leaflet of the membrane. The wedge shaped ganglioside molecules in the membrane would occupy a large surface area and thus perturb the packing of the phospholipid acyl chains. This would conspicuously enhance the fluidity of the bilayer region near the exoplasmic surface. The higher interfacial polarity of gangliosides may be responsible for the increased hydration in this region of the lipid bilayer. Mehlhorn et al. [48] have demonstrated that glycolipids with different head groups do not show a detectable difference in organization of lipids in the central region of the membrane hydrophobic interior as probed by the order parameter of a spin label. On the other hand ^{2}H-NMR studies by Grant and co-workers show that the length of the fatty acyl chain of glycosphingolipid is an important determinant of the orientational mobility of lipids in the central core region of the bilayer [49,50]. The gradient of the order parameter with respect to the distance from the sugar headgroup for the 24-carbon glycolipid was comparable to that for the 18-carbon analogue to the depth of C_{14}; beyond this point its slope became sharply reduced suggesting a more restricted motion of acyl chains in the central region of the bilayer consisting of a 24-carbon fatty acyl chain. This has been attributed to the interdigitation of glycosphingolipid fatty acid chains with the lipids in the cytoplasmic leaflet of the bilayer. In agreement to the above mentioned reports we observed the ordering effect of gangliosides in the central region of the bilayer as probed by DPH, however, the interdigitation of gangliosides with lipids in the cytoplasmic leaflet can not be ascertained with the present data.

We observed that BBG incorporation enhanced the permeability of PC-12 cell membranes to cations. These results are in agreement with Sarti et al. [51] who have shown that gangliosides incorporated into the cytochrome C containing phospholipid vesicles stimulate the activity of the enzyme by permeabilizing the membrane. A BBG-induced increase in the Ca^{2+} permeability of plasma membranes of various cells has been

reported [19]. One possibility is that the defects created due to the disturbance in the packing of phospholipids in the bilayer may be responsible for this increase in permeability. Also the ganglioside incorporation may cause a lateral phase separation of lipids and thus form hydrophilic pores in the membrane, however, the present data are unable to support this proposition. Although the generalized polarization spectra of laurdan has been shown to manifest the coexistence of lipid domains in gel and liquid crystalline phases in phospholipid vesicles [44,47], recently Baggatolli et al. [52] have reported that laurdan *GP* is unable to recognize the coexisting phases in pure glycolipid aggregates. Thus the presence of ganglioside microdomains in the plasma membrane of BBG treated cells is not ruled out. However, these propositions appear to be less likely as no change was observed in the polarity of the inner core of the membrane and the flux rates for the three ions were markedly different. A more probable proposition is that the physiological processes, such as membrane depolarization and consequent activation of voltage gated ion channels give rise to the cation fluxes induced by BBG. Further experiments are required to ascertain this. Potentiation of L-type Ca^{2+} channel activity by GM_1 in PC-12 cells has been reported [23].

Our data demonstrate that exogenously incorporated gangliosides produce significant structural and dynamic changes in the lipid bilayer of the cell membrane. The enhanced fluidity and hydration of the lipid bilayer could be crucial in regulation of lipid–protein interactions and thus modify the activity of membrane proteins. Exogenously added gangliosides potentiate the neurotrophic effects of nerve growth factor in PC-12 cells. This potentiation is thought to be mediated by GM_1-induced dimerization of the cell surface glycoprotein receptor Trk leading to the activation of a Ca^{2+}-dependent tyrosine kinase [15]. The fluidization of the outer leaflet of the plasma membrane by GM_1 may facilitate the dimerization of the receptor molecule. The physical changes in the exoplasmic leaflet of the plasma membrane reported here could be an important step in modulation of signaling events triggered at the cell surface.

Acknowledgements

The authors are thankful to the Human Brain Tissue Repository for Neurobiological Studies (Brain Bank), NIMHANS, Bangalore, India for the use of fluorescence microscope. This work was supported by the Council of Scientific and Industrial Research, New Delhi, India.

References

[1] H.A. Hansen, J. Holmgren, L. Svennerholm, Proc. Natl. Acad. Sci. USA 74 (1977) 3782.
[2] R.W. Ledeen, J. Supramol. Struct. 8 (1978) 1.
[3] P.H. Fishman, R.M. Brady, E.B. Hom, J. Moss, J. Lipid Res. 24 (1980) 1002.
[4] R.T.C. Huang, E. Dietsch, FEBS Lett. 281 (1991) 39.
[5] H.E. Saqr, D.K. Pearl, A.J. Yates, J. Neurochem. 61 (1993) 395.
[6] G. Ferrari, M. Fabris, A. Gorio, Dev. Brain Res. 8 (1983) 215.
[7] L. Facci, A. Leon, G. Toffano, S. Sonnino, R. Ghidoni, G. Tettamanti, J. Neurochem. 42 (1984) 299.
[8] P. Doherty, S.V. Ashton, D. Skaper, A. Leon, F.S. Walsh, J. Cell Biol. 17 (1992) 1093.
[9] J.R. Sparrow, B. Graftein, Exp. Neurol. 77 (1982) 230.
[10] C.L. Schengrund, Brain Res. Bull. 24 (1990) 131.
[11] M. Favaron, H. Manev, H. Alho, B. Bertolino, A.G. Ferret, E. Costa, Proc. Natl. Acad. Sci. USA 85 (1988) 7531.
[12] D. Erausquin, H. Manev, A. Guidotti, E. Costa, G. Brooker, Proc. Natl. Acad. Sci. USA 87 (1990) 8017.
[13] G. Ferarri, B.L. Anderson, R.M. Stephens, D.R. Kaplan, L.A. Greene, J. Biol. Chem. 270 (1995) 3074.
[14] S.I. Hakomori, J. Biol. Chem. 265 (1990) 18713.
[15] T. Farooqui, T. Franklin, D.K. Pearl, A.J. Yates, J. Neurochem. 68 (1997) 2348.
[16] G. Wu, K.K. Vaswani, Z.-H. Lu, L.W. Ledeen, J. Neurochem. 55 (1990) 484.
[17] B.S. Hilbush, J.M. Levine, J. Biol. Chem. 267 (1992) 24789.
[18] A.J. Yates, J. VanBrocklyn, H.E. Saqr, Z. Guan, B.T. Stokes, M.S. O'Dorisio, Exp. Cell Res. 204 (1993) 38.
[19] S.D. Isasi, I.D. Bianco, G.D. Fidelio, Life Sci. 57 (1995) 449.
[20] A.J. Yates, J.D. Walters, C.L. Wood, J. Neurochem. 53 (1989) 162.
[21] K.K. Vaswani, G. Wu, R.W. Ledeen, J. Neurochem. 55 (1990) 492.
[22] T.M. Dawson, K. Hung, V.L. Dawson, J.P. Steiner, S.H. Snyder, Ann. Neurol. 37 (1995) 115.
[23] B.S. Hilbush, J.M. Levine, Proc. Natl. Acad. Sci. USA 88 (1991) 5616.

[24] T. Mutoh, A. Tokuda, T. Miyadai, M. Hamaguchi, N. Fujiki, Proc. Natl. Acad. Sci. 92 (1995) 5087.
[25] G. Rimon, E. Hanski, S. Braun, Dummy Levitski, Nature 267 (1978) 394.
[26] R. Salesse, J. Garnier, F. Leterrier, D. Davaloose, J. Viret, Biochemistry 21 (1982) 1581.
[27] A.H. Parola, Mammalian membranes: structure and function, in: Biomembranes, Physical Aspects, Balaban Publishers VCH, New York, 1993.
[28] P. Casey, Science 268 (1995) 221.
[29] E. Alfahel, A. Korngreen, A.H. Parola, Z. Priel, Biophys. J. 70 (1996) 1045.
[30] K. Simon, E. Ikonen, Nature 387 (1997) 569.
[31] E. Bertoli, M. Masserini, S. Sonnino, R. Ghidoni, B. Cestaro, G. Tettamanti, Biochim. Biophys. Acta. 467 (1981) 196.
[32] T. Uchida, Y. Nagai, Y. Kawasaki, N. Wakayama, Biochemistry 20 (1981) 162.
[33] C. Usai, M. Robello, F. Gambale, C. Marchetti, J. Membrane Biol. 82 (1984) 15.
[34] M. Shinitzky, M. Inbar, J. Mol. Biol. 85 (1974) 603.
[35] H.R. Petty, C.D. Niebylski, J.W. Francis, Biochemistry 26 (1987) 6340.
[36] T. Parasassi, M. Di Stefano, G. Ravangan, O. Sapora, E. Gratton, Exp. Cell Res. 202 (1992) 432.
[37] M. Sharma, P.G. Joshi, N.B. Joshi, Biochim. Biophys. Acta. 1323 (1997) 272.
[38] J.R. Lakowicz, Principles of Fluorescence Spectroscopy, Plenum Press, New York 1983.
[39] K. Hildenbrand, C. Nicolan, Biochim. Biophys. Acta. 553 (1979) 365.
[40] K. Kinosita, K. Kataoka, Y. Kimura, O. Gotoh, R. Ikegami, Biochemistry 20 (1981) 4270.
[41] P.G. Joshi, S. Mishra, Brain Res. 597 (1992) 108.
[42] J.G. Kuhry, P. Fonteneau, G. Duportail, C. Maechling, G. Laustriat, Cell Biophys. 5 (1983) 129.
[43] C.L. Grimellec, G. Friedlander, M. Giocondi, Am. J. Physiol. 255 (1988) F22.
[44] T. Parasassi, G. De Stasio, G. Ravangan, A. d'Ubaldo, E. Gratton, Biophys. J. 57 (1990) 1179.
[45] T. Parasassi, G. De Stasio, G. Ravangan, M.R. Rusch, E. Gratton, Biophys. J. 60 (1991) 179.
[46] R. Fiorini, G. Curatola, A. Kantar, P.L. Giorgi, E. Gratton, Photochem. Photobiol. 57 (1993) 438.
[47] T. Parasassi, M. Di Stefano, M. Loiero, G. Ravangan, E. Gratton, Biophys. J. 66 (1994) 120.
[48] I.E. Mehlhorn, K.R. Barber, E. Florio, C.W.M. Grant, Biochim. Biophys. Acta 986 (1989) 281–289.
[49] D. Lu, M.R. Morrow, C.W.M. Grant, Biochemistry 32 (1993) 290–297.
[50] M.R. Morrow, D. Singh, C.W.M. Grant, Biophys. J. 68 (1995) 179.
[51] P. Sarti, G. Antonini, F. Malatesta, B. Vallone, M. Brunori, M. Masserini, P. Palestini, G. Tettamanti, Biochem. J. 267 (1990) 413.
[52] L.A. Baggatolli, B. Maggio, F. Aguilar, C.P. Sotomayor, G.D. Fidelio, Biochim. Biophys. Acta 1325 (1997) 80.